Experiment [4] in our pressure range is represented by the solid line in Fig. 1, with the scale of the Faraday dark space given by $pL = a(pR)^2$, $a \approx 0.14\ (\text{torr}\cdot\text{cm})^{-1}$. The proportionality observed between L and pR^2 [compare (13)] is governed by the dependence of F on p and R, with G independent of those parameters [see (9)]. It is not surprising that there is an anomalously large dark space only in helium [4] because already for Ne and particularly for the heavier gases, the lower pressure bound for the model increases in proportion to T/(E/p), as (11) shows, from 10 torr for helium (R = 2 cm, nominal boundary for model L ≈ 2.5R) to more than 50 torr, where bulk recombination becomes considerable for the inert gases beginning with Ne.

LITERATURE CITED

1. Yu. P. Raizer, Gas-Discharge Physics [in Russian], Nauka, Moscow (1987).
2. Yu. M. Kagan, C. Cogen, and P. Avivi, "Faraday dark space of a He glow discharge," J. Appl. Phys., 63, No. 1 (1988).
3. V. A. Granovskii, Electric Currents in Gases: Steady-State Current [in Russian], Nauka, Moscow (1971).
4. A. Rutcher and Ch. Wilke, "Investigation of very long Faraday dark spaces," 11th Intern. Conf. on Phenomena in Ionized Gases, Prague (1973), contr. pap.
5. D. I. Vysikailo, "Ambipolar drift," Teplofiz. Vys. Temp., 23, No. 4 (1985).
6. Yu. S. Akishev, D. I. Vysikailo, A. P. Napartovich, and V. V. Ponomarenko, "A study on a quasistationary discharge in nitrogen," Teplofiz. Vys. Temp., 18, No. 2 (1980).
7. J. Berlande, M. Cheret, R. Deloche, et al., "Pressure and electron density dependence of the electron—ion recombination coefficient in helium," Phys. Rev., 1A, No. 3 (1970).
8. R. Deloche, A. Confalone, and M. Cheret, "Mesure en fonction de la pression, de la variation du coefficient de recombination electron-ion, dans l'helium faiblement ionisé, en regime de relaxation," C. R. Acad. Sci., 267, No. 18 (1968).
9. B. M. Smirnov, Atomic Collisions and Elementary Processes in Plasmas [in Russian], Nauka, Moscow (1988).
10. A. Van Engel, Ionized Gases [Russian translation], Fizmatgiz, Moscow (1959).
11. I. McDaniel, Collision Processes in Ionized Gases [Russian translation], Mir, Moscow (1967).
12. W. Schottky, "Diffusions-Theorie der positiven Säul," Phys. Z., 25, No. 23 (1924).

MHD DECELERATION AND HEAT TRANSFER FOR A SPHERE IN A SUPERSONIC FLOW OF PARTIALLY IONIZED GAS

V. V. Gubin and V. A. Shuvalov

UDC 533.95:538.4:537.523

The inherent magnetic field has a substantial effect on the structure of the perturbed zone at the surface of a body in a supersonic low-density plasma [1]. The inherent field of the body may be due to a set of currents or to permanent magnets. The perturbations caused by that field affect the functional and dynamic characteristics in the interaction with the flow. An approximate numerical analysis [2, 3] and experiment [4, 5] indicate effective MHD retardation in such a flow. It is desirable to examine MHD control of heat transfer and the aerodynamic characteristics.

Measurements are reported here on the MHD retardation and heat transfer as affected by the direction of the inherent field of the body $\mathbf{H}$ with respect to the incident velocity vector $\mathbf{U}_\infty$. MHD control is possible for the aerodynamic performance and convective heat transfer for a sphere if the field is rotated with respect to the velocity vector.

1. The experiments were performed with a plasma gas-dynamic system in partially ionized nitrogen generated by a gas-discharge accelerator, in which the ionization was provided by

---

Dnepropetrovsk. Translated from Zhurnal Prikladnoi Mekhaniki i Tekhnicheskoi Fiziki, No. 1, pp. 15-19, January-February, 1991. Original article submitted May 15, 1989; revision submitted July 10, 1989.

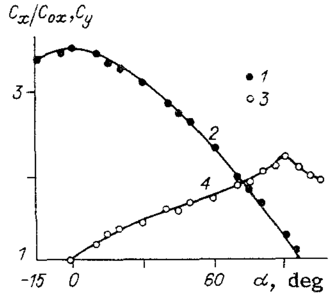

Fig. 1

electron impact and plasma self-acceleration. The accelerated plasma entered the working chamber, where the residual-gas pressure was ~10^{-5} Pa. The pumping was provided by an AVÉD-40/800M discharge pump and TMN-500 turbomolecular one. The plasma flow parameters were monitored at working pressures in the chamber of ~10^{-1}-10^{-3} Pa by means of mobile probes and a multielectrode analyzer probe. The voltage—current characteristics and the probe—current derivatives were measured automatically. The errors in the individual characteristics did not exceed ±2%. The plasma potential was determined by the second-derivative method and also from the electron branch in the probe characteristic plotted on a semilog scale. The circuit for measuring the probe current derivatives enabled one to record also the plasma noise in the probe circuit, which made it possible to check the accuracy in determining the plasma potential: the maximum plasma noise level corresponds to the space potential. The plasma potential was identified also from the point at which the voltage—current curves diverge for cold and heated thermoprobes. The spread in the plasma potentials was not more than ±4%, which characterizes the fairly high accuracy in measuring the ion energies W_i. These energies were calculated on the assumption that the accelerating potential is equal to the potential difference between the anode in the source and the local plasma potential, and these W_i then agreed satisfactorily with those from the multielectrode analyzer probe. The spread in the W_i did not exceed ±4.5%.

To raise the accuracy in determining the charged-particle concentration, the probe measurements were combined with UHF diagnosis by means of a 3 cm interferometer. The local concentrations found from the electron currents for planar and cylindrical probes at the point on the characteristic corresponding to the plasma potential agreed satisfactorily with the UHF measurements. The orientation of the model with respect to the incident velocity vector was monitored with a single cylindrical probe made of molybdenum wire 0.04 mm in diameter and 2.3 mm long. The peak in the ion current recorded by it on rotation around the vertical and horizontal axes corresponds to the orientation along the flow and enables one to estimate the deviation from isothermal behavior in it [6].

2. The measurements were made in a section of the jet having a uniform parameter distribution: external magnetic field $H \lesssim 2$ Oe, $W_i \approx 10$-60 eV, and charged-particle concentration $N_\infty \approx 10^8$-10^{11} cm^{-3}. The source of the inherent magnetic field was a solenoid having an outside diameter of 50 mm, internal diameter 20 mm, and length 34 mm. Figure 6 in [7] shows the distributions of the axial and radial-azimuthal field components. The model was a sphere 65 mm in diameter made of hard paper. The strength of the inherent field was such that a locally magnetized plasma was produced near the body. When the weak magnetic field was applied, the floating negative potential at the surface shifted to the positive side. Subsequently, as the field strengthened, the surface potential remained almost unaltered. For $N_\infty \approx 10^8$-10^{11} cm^{-3} in the incident flow and fields at the surface of a metal sphere 65 mm in diameter, $H_W \approx 0$-150 Oe resulted in a maximum change in the negative floating potential of ~12%, and a minimum of 4%. The plasma interacts with the negatively charged and magnetized body. The structure in the perturbed zone in axisymmetric and planar flow around a large insulating body ($R/\lambda_d \gtrsim 10^2$, λ_d the Debye radius for the unperturbed plasma, and R the characteristic dimension of the body) is identical with the structure of the perturbed zone around a negatively charged body. Changes in the range ~4-12% in the surface potential have a negligible effect on the resistance of a large negatively charged body [4].

The body enclosed the solenoid mounted on a rotating support and acted as the sensing element in a microbalance. The force exerted on the sphere with its inherent field was measured automatically, in which the resistance as a function of field strength was recorded by an XY recorder.

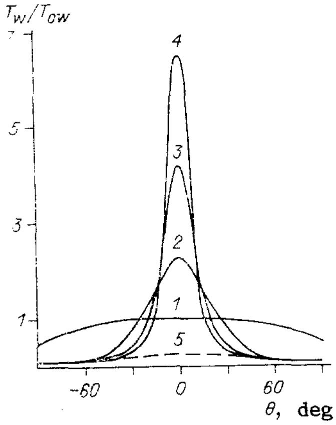

Fig. 2

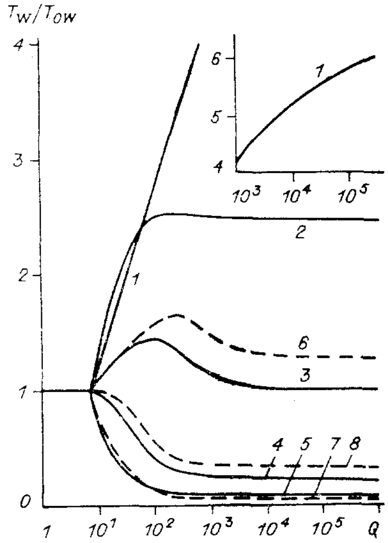

Fig. 3

Figure 1 shows how the frontal resistance coefficient C_x and the lift coefficient C_y for a sphere vary when **H** is rotated relative to $\mathbf{U}_\infty$. Points 1 are for C_x and points 3 for C_y with $\xi \approx 3.2$; $U_\infty \approx 11.2$ km/sec and $Q \approx 2.5 \cdot 10^3$, which can be approximated with an error of not more than ±2% by

$$C_x/C_{0x} \approx 1 + \xi^{0,8}(\cos\alpha + 0.134|\sin\alpha|(|\sin\alpha| - \cos\alpha))$$

(curve 2) and

$$C_y = C_{0y} + 1 \approx 1 + \xi^{0,2}(\sin\alpha - |\cos\alpha|(1 - |\cos\alpha|))$$

(curve 4). Here C_{0x} and C_{0y} are those coefficients in the absence of the field, $\xi = \beta e U_\infty P_m / W_i$; $\beta \approx 2.17$ cm^{-2}, e charge, P_m magnetic moment of the solenoid, $Q = \sigma_\infty H_W{}^2 R/\rho_\infty U_\infty$ magnetic interaction parameter, σ_∞ electrical conductivity, ρ_∞ density in the unperturbed flow, and α the angle between **H** and $\mathbf{U}_\infty$. Rotating the inherent field affects the aerodynamic characteristics in a fashion somewhat equivalent to the interaction of jets emerging from the front surface of a body of rotation [8] but with the difference that in the case of MHD interaction, the particles reflected by the inherent field make a contribution to the force on the body substantially larger than that from those colliding directly with it.

3. The equatorial plane in the insulating sphere was fitted with miniature thermocouples to examine how rotating the field affected the heat transfer. Figure 2 shows the temperature distribution T_W/T_{0W} at the surface as a function of the angle of attack θ for $\alpha = 0$. Here $T_{0W} = T_W(\theta, H_W = 0)$, and curve 1 characterizes that distribution for $U_\infty \approx 11.2$ km/sec and $H_W = 0$, while 2-4 correspond to $Q \approx 5 \cdot 10^1$; $5 \cdot 10^3$; $2 \cdot 10^7$; curve 5 is the radiative heating from the plasma emission for $N_\infty \approx 10^{10}$ cm^{-3}. As the field strengthens, the MHD interaction parameter rises, and the heat fluxes become localized: increase in the range $\theta \approx$ 0-25° and decrease over the rest of the surface. Figure 3 confirms this from T_W/T_{0W} as a function of field and Q at points on the surface [1-5) θ = 0, α = 0, 15, 30, 60, 90°; 6-8) θ = 15, 30, 45°, α = 0]. There is a certain increase in T_W/T_{0W} for $10^1 \lesssim Q \lesssim 10^3$ due to slight screening of the $\theta \lesssim 25°$ surface by the field. The charged-particle flux slides over the surface for $\theta \lesssim 25°$. As the field and Q increase, the Larmor radius decreases, and the screening at $\theta \lesssim 25°$ is accentuated, with the heat flux decreasing. As the angle between **H** and $\mathbf{U}_\infty$ alters, the polar points shift and there are changes in the flow and in the charged-particle distribution. The flows corresponding to $\mathbf{H} \parallel \mathbf{U}_\infty$ $(\alpha = 0)$ and $\mathbf{H} \perp \mathbf{U}_\infty$ $(\alpha = 90°)$ are shown in parts a and b of Fig. 4. We used a short cylinder, since there are more prominent features in the charged-particle distribution near a cylinder for the same field strength at the axis and with identical structure in the perturbed zone. That structure and the charged-particle distribution at the surface may be seen for these cases from Fig. 6 in [1] and Fig. 7 in [7]. Figure 5 shows the changes in T_W/T_{0W} at the surface for various solenoid orientations with $Q \approx 2 \cdot 10^7$: curves 1-6 correspond to points with θ = 0, 15, 30, 45, 75, 90°, correspondingly, while curve 7 characterizes the temperature distribution at the sur-

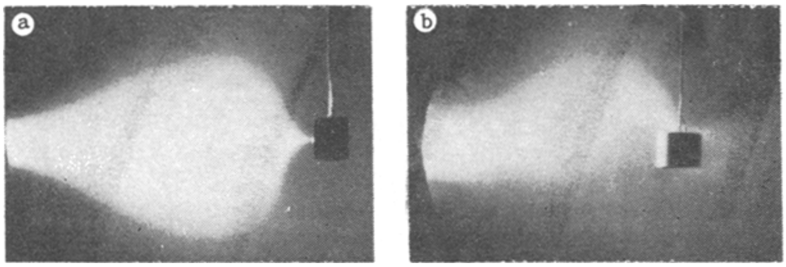

Fig. 4

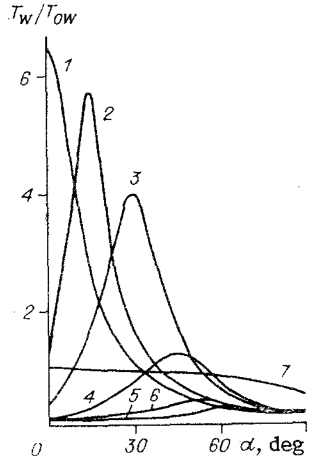

Fig. 5

face for $H_W = 0$. It is thus possible to reduce the heat flux at the critical point for $\alpha \gtrsim 60°$ and to control and redistribute the flux in a supersonic plasma.

The temperature and particle-density distributions at the surface for $\mathbf{H} \parallel \mathbf{U}_\infty$ ($\alpha = 0$, Fig. 4a) correspond to an axisymmetric MHD interaction region ahead of the body, in which currents flow. The increase in heat flux at the critical point ($\theta = 0$) is due to the increase in the charged-particle density, which accentuates the focusing at the axis. For $\mathbf{H} \perp \mathbf{U}_\infty$ ($\alpha = 90°$, Fig. 4b), the perturbed zone has only one symmetry plane, which is perpendicular to the axis of the solenoid. The heat flux here is reduced because a cavity is formed: the plasma hardly penetrates the region ahead of the body. Also, with the Hall parameter $\omega\tau \gtrsim 1$, there is marked anisotropy in the transport coefficients: perpendicular to the field, they are reduced by a factor of $(1 + \omega^2\tau^2)^{-1}$ [9], which also reduces the heat flux.

One can adjust the perturbed-zone structure, the flow, and the charged-particle distribution and provide effective control of the forces and heat interaction for a magnetized body in a flow of partially ionized gas.

LITERATURE CITED

1. V. A. Shuvalov, "Effects of an internal magnetic field on the structure of the perturbed zone around a body in a low-density plasma flow," Zh. Tekh. Fiz., 54, No. 6 (1984).
2. S. Y. Chen, "Magnetic hypersonic flow near the stagnation point and Reynolds number," J. Spacecr. Rockets, 6, No. 8 (1969).
3. R. Nowak, S. Krane, R. Porter, et al., "Magnetogasdynamic re-entry phenomena," J. Spacecr. Rockets, 4, No. 11 (1967).
4. V. A. Shuvalov, "Surface-potential and inherent-field effects on the resistance of a body in a supersonic flow of low-density partially ionized gas," Zh. Prikl. Mekh. Tekh. Fiz., No. 3 (1986).
5. V. V. Gubin and V, A. Shuvalov, "The resistance of a body containing a magnetic field in a supersonic flow of partially ionized gas," Zh. Prikl. Mekh. Tekh. Fiz., No. 1 (1990).
6. G. R. Sanmarting, "End effect in Langmuir probe response under ionosphere satellite conditions," Phys. Fluids, 15, No. 6 (1972).
7. V. A. Shuvalov, "Structure of the plasma formations at the surface of a cylinder in a flow of partially ionized gas," Zh. Prikl. Mekh. Tekh. Fiz., No. 4 (1984).
8. B. L. Zhirnikov and K. I. Petrov, "Interactions with an opposite flow for jets emerging from the frontal surface of a body of rotation," in: Current Aeromechanics Topics [in Russian], Mashinostroenie, Moscow (1987).
9. S. I. Braginskii, "Transport phenomena in plasmas," in: Aspects of Plasma Theory [in Russian], Issue 1, Gosatomizdat, Moscow (1963).